Structure of the $Li_4Ti_5O_{12}$ anode during charge-discharge cycling

Wei Kong Pang,[1,2] Vanessa K. Peterson,[1,a)] Neeraj Sharma,[3] Je-Jang Shiu,[4] and She-huang Wu[4]
[1]*Australian Nuclear Science and Technology Organization, Locked Bag 2001, Kirrawee DC, NSW 2232, Australia*
[2]*Faculty of Engineering, School of Mechanical, Materials, and Mechatronic Engineering, Institute for Superconducting and Electronic Materials, University of Wollongong, NSW 2522, Australia*
[3]*School of Chemistry, University of New South Wales, Sydney, NSW 2052, Australia*
[4]*Department of Materials Engineering, Tatung University, No.40, Sec. 3, Zhongshan N. Rd., Taipei City 104, Taiwan*

(Received 8 September 2014; accepted 30 September 2014)

The structural evolution of the "zero-strain" $Li_4Ti_5O_{12}$ anode within a functioning Li-ion battery during charge–discharge cycling was studied using *in situ* neutron powder-diffraction, allowing correlation of the anode structure to the measured charge–discharge profile. While the overall lattice response controls the "zero-strain" property, the oxygen atom is the only variable in the atomic structure and responds to the oxidation state of the titanium, resulting in distortion of the TiO_6 octahedron and contributing to the anode's stability upon lithiation/delithiation. Interestingly, the trend of the octahedral distortion on charge–discharge does not reflect that of the lattice parameter, with the latter thought to be influenced by the interplay of lithium location and quantity. Here we report the details of the TiO_6 octahedral distortion in terms of the O–Ti–O bond angle that ranges from 83.7(3)° to 85.4(5)°. © *2014 International Centre for Diffraction Data.*
[doi:10.1017/S0885715614001067]

Key words: Li-ion battery, $Li_4Ti_5O_{12}$, neutron diffraction, phase evolution

I. INTRODUCTION

Li-ion batteries (LIBs) have higher-energy density, portative design, and longer lifetime than comparable battery technologies (Tarascon and Armand, 2001). Spinel $Li_4Ti_5O_{12}$, a so-called zero-strain insertion material, has been commercialized as an anode material because of its exceptionally high rate performance, excellent cycling stability, and Li-insertion electrochemistry with formal potential of 1.55–1.56 V versus Li^+/Li (Ohzuku *et al.*, 1995; Cho *et al.*, 2001; Ronci *et al.*, 2002). Generally speaking, Li-(de)intercalation in $Li_{4+z}Ti_5O_{12}$ ($z = 0$–3) proceeds through a two-phase reaction, as given in Eq. (1), resulting in flat plateaus in the charge and discharge curves.

$$(\mathrm{Li})^{8a}(\mathrm{Li}_{1/3}\mathrm{Ti}_{5/3})^{16d}\mathrm{O}_4^{32e} + xe^- + x\mathrm{Li}^+ \xrightarrow{\sim 1.55\ \mathrm{V}} (1-x)(\mathrm{Li})^{8a}(\mathrm{Li}_{1/3}\mathrm{Ti}_{5/3})^{16d}\mathrm{O}_4^{32e} + x(\mathrm{Li}_2)^{16c}(\mathrm{Li}_{1/3}\mathrm{Ti}_{5/3})^{16d}\mathrm{O}_4^{32e} \quad (1)$$

$(\mathrm{Li})^{8a}(\mathrm{Li}_{1/3}\mathrm{Ti}_{5/3})^{16d}\mathrm{O}_4^{32e}$ and $(\mathrm{Li}_2)^{16c}(\mathrm{Li}_{1/3}\mathrm{Ti}_{5/3})^{16d}\mathrm{O}_4^{32e}$, where the site multiplicity and Wyckoff letter is shown in superscript, crystallize in the $Fd\bar{3}m$ space group. 1/6th of 16*d* sites are occupied by the "electrochemically inert" Li, with the remainder occupied by Ti (see Figure 1). The "electrochemically active" Li occupies the tetrahedral 8*a* sites of the $Li_4Ti_5O_{12}$ lattice and is repositioned together with the newly inserted Li at the octahedral 16*c* sites to form stable $Li_7Ti_5O_{12}$ upon Li-intercalation. The Li-(de)intercalation of $Li_4Ti_5O_{12}$ is also reported to occur *via* the following solid-solution reaction [Eq. (2)]:

$$(\mathrm{Li})^{8a}(\mathrm{Li}_{1/3}\mathrm{Ti}_{5/3})^{16d}\mathrm{O}_4^{32e} + xe^- + x\mathrm{Li}^+ \xrightarrow{\sim 1.55\ \mathrm{V}} (\mathrm{Li}_{1-y})^{8a}(\mathrm{Li}_{x+y})^{16c}(\mathrm{Li}_{1/3}\mathrm{Ti}_{5/3})^{16d}\mathrm{O}_4^{32e} \quad (2)$$

where $z, y \leq 1$.

The phase transition between $Li_4Ti_5O_{12}$ and $Li_{4+z}Ti_5O_{12}$ ($Li_7Ti_5O_{12}$ in the two-phase mechanism), as outlined in Eqs. (1)–(2), involves a <0.1% change in the lattice volume. The Li accommodated by the anode results in changes to the Ti oxidation state, affecting the structure of the TiO_6 octahedral framework (Figure 1).

Given that the underlying mechanism of the phase transitions upon lithiation remains controversial and, importantly, may control the performance of the $Li_4Ti_5O_{12}$ anodes, we have studied the $Li_{4+z}Ti_5O_{12}$ structure in detail during battery cycling. Neutron powder-diffraction (NPD) data were collected during the non-equilibrium charge and discharge of a $LiFePO_4$‖ $Li_4Ti_5O_{12}$ battery within the 1.0–3.0 V window (versus $Li_4Ti_5O_{12}$). While the details of the Li diffusion within the $Li_{4+z}Ti_5O_{12}$ structure is thought to control the lattice response and is discussed in detail elsewhere in work focusing on particle-size differences (Pang *et al.*, 2014a), here we focus on the structural details and distortion of the TiO_6 octahedron. In this work, we extract and discuss the Ti–O bond length and O–Ti–O angle that dictate the size of the TiO_6 unit and assist in maintaining the stability of the anode during lithiation and delithiation.

a)Author to whom correspondence should be addressed. Electronic mail: vanessa.peterson@ansto.gov.au

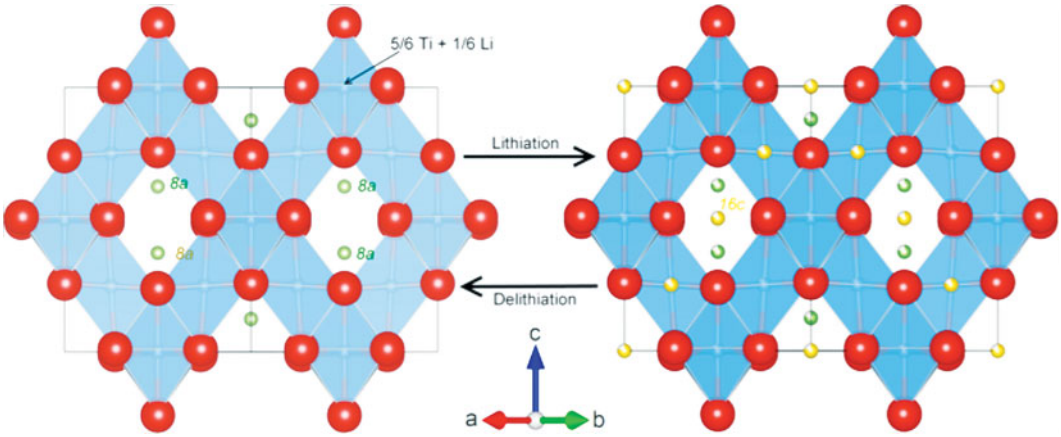

Figure 1. (Color online) (Left) Crystal structure of the as-prepared $Li_4Ti_5O_{12}$ as refined using high-resolution NPD data. Li (8*a*) is shown in green, O in red, and mixed Ti/Li sites in light blue. For clarity, Li and Ti sites are shown as fully occupied. Li at 16*c* sites (yellow) are also shown in the $Li_{4+z}Ti_5O_{12}$ structure (right) following lithiation.

II. EXPERIMENTAL

A. Preparation

$LiFePO_4$ cathode powder was provided by Tatung Fine Chemicals Co., Taiwan. $Li_4Ti_5O_{12}$ anode powder was prepared *via* a sol–gel method using Li acetate (98%, Acros) and titanium butoxide (98.0%, Acros). The stoichiometrically mixed powders were dissolved in an adequate amount of ethanol (99.5%, Shimakyu) and the solution aged for 3 h to form a white-colored gel. The resulting gel was heated at 80 °C to yield an organic precursor with a fine, white powder-product obtained by heat-treating in air at 800 °C for 4 h.

A purpose designed $LiFePO_4$|| $Li_4Ti_5O_{12}$ pouch-type battery (Figure 2) was used in the collection of *in situ* NPD data. The $LiFePO_4$ cathode was prepared by casting a slurry of the active materials (80 wt%), acetylene black (10 wt%), and polyvinylidene difluoride (PVDF) binder (10 wt%) onto an Al foil. The $Li_4Ti_5O_{12}$ anode was prepared using the same procedure, but with $Li_4Ti_5O_{12}$ powder as the active material. The loading ratio between the anode and cathode was designed to be ~4:6 by weight. The electrodes were cut into 1×4 cm strips. Immobilon-P PVDF membrane (Millipore) was used as a separator because of its lower hydrogen content relative to the conventionally used the Celgard membrane, where the strong incoherent neutron-scattering of hydrogen is detrimental to the NPD signal. The $LiFePO_4$||$Li_4Ti_5O_{12}$ battery was prepared by stacking 30 anode/separator/cathode assemblies with a parallel connection. The stack was placed in an Ar-filled glove box for 24 h and then wrapped in a polypropylene-coated Al foil to form a pouch. Prior to the *in situ* NPD experiment, deuterated electrolyte-solution (1 M lithium hexafluorophosphate (99.99%, Sigma-Aldrich) in a 1:1 volume ratio of deuterated dimethyl carbonate (99.5%, Novachem) to deuterated ethylene carbonate (98%, Novachem) was injected into the pouch, which was heat-sealed under Ar. After 1 day of wetting, the battery was used in the *in situ* NPD experiment. During the *in situ* NPD experiment the pouch-type battery was cycled galvanostatically using a potentiostat/galvanostat (Autolab PG302N) at currents of 11 mA (theoretically equivalent to 0.1 °C) for 1 cycle between 1.0 and 3.0 V (versus $Li_4Ti_5O_{12}$).

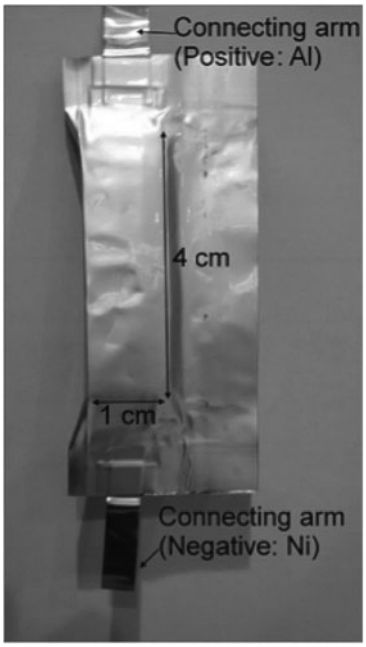

Figure 2. Pouch cell used in the *in situ* NPD experiment.

B. Data collection and analysis

High-resolution NPD data of the as-prepared $Li_4Ti_5O_{12}$ sample were collected using ECHIDNA, the high-resolution neutron powder-diffractometer at the Open Pool Australian Light-water (OPAL) research reactor at the Australian Nuclear Science and Technology Organisation (ANSTO; Liss *et al.*, 2006). The neutron beam wavelength was 1.6214 (4) Å, determined using the $La^{11}B_6$ NIST standard reference material 660b. NPD data were obtained in the 2θ angular range 4–164° with a step size of 0.125°. Rietica ver. 1.77 (Hunter, 1998) was used to perform Rietveld analysis of the high-resolution NPD data. The refinable parameters included the background coefficients, zero-shift, peak shape parameters, lattice parameters, O positional parameter, and isotropic atomic displacement parameters. Micrographs of the as-prepared $Li_4Ti_5O_{12}$ were collected using field-emission scanning electron microscopy (SEM) with a SU8000

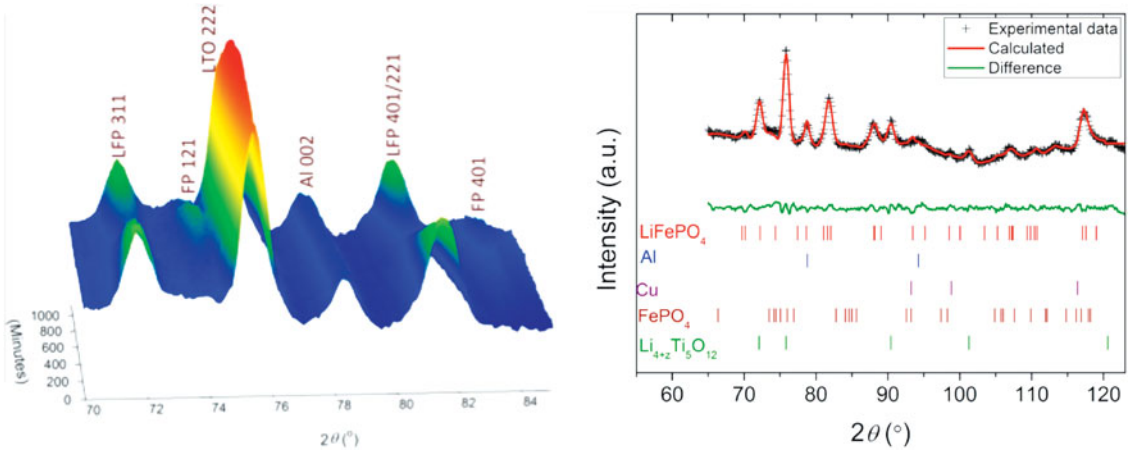

Figure 3. (Color online) Waterfall plot (left) of a collection of NPD patterns shown for a restricted 2θ range taken during battery charge and discharge. Labels are phase reflections for $LiFePO_4$ (LFP), $FePO_4$ (FP), $Li_{4+z}Ti_5O_{12}$ (LTO), and Al. A typical Rietveld-refinement profile before cycling (right) is also shown. The figures-of-merit for the refinements were in the range $\chi^2 = 3.9–8.95$, $R_{wp} = 14.3–17.1$, and $R_B = 1.0–3.9\%$.

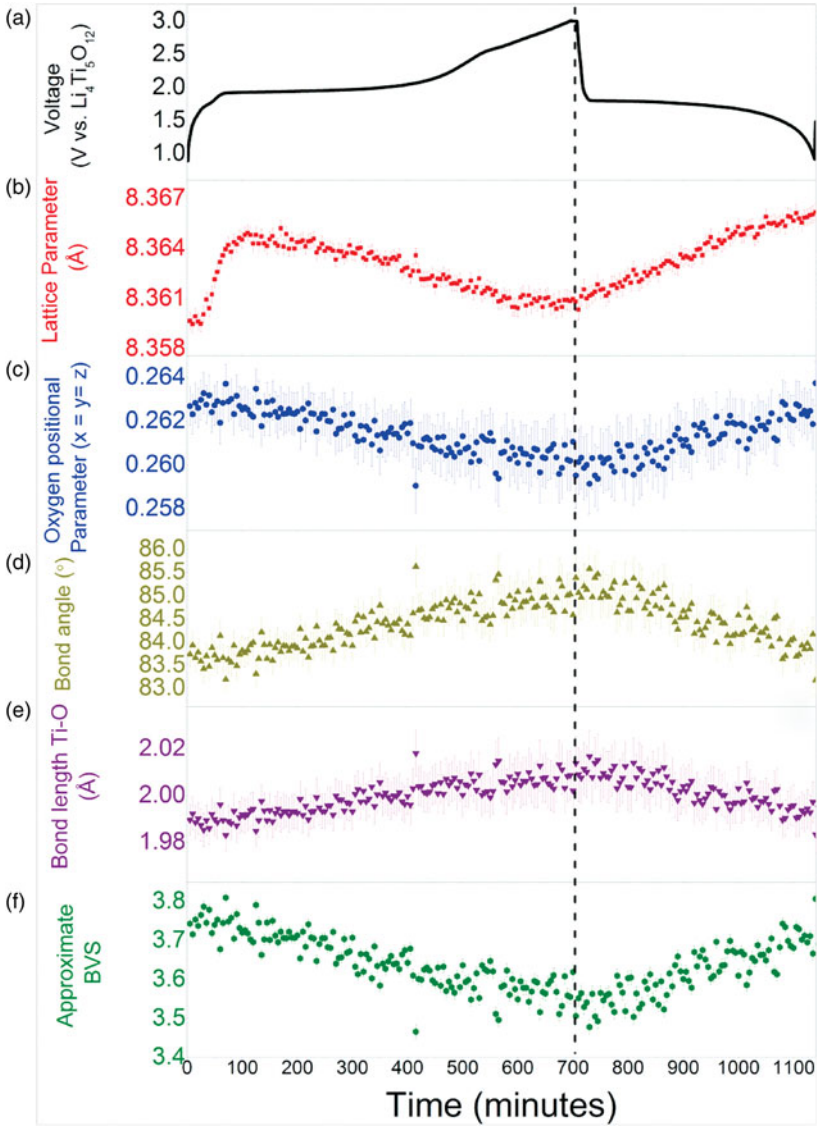

Figure 4. (Color online) (a) Charge–discharge profile, (b) refined anode lattice-parameter, (c) refined oxygen positional-parameter, (d) α bond-angle, and (e) Ti–O bond length, during battery charge and discharge. The titanium oxidation-state in (f) is estimated using the approximate BVS method.

(Hitachi, Japan). All observations were carried out without a conductive coating under a 10 kV acceleration voltage.

In situ NPD data of the $LiFePO_4$||$Li_4Ti_5O_{12}$ battery were collected using WOMBAT (Studer *et al.*, 2006), the high-intensity neutron powder-diffractometer at the OPAL research reactor at ANSTO. WOMBAT features an area detector that continuously covers 120° in 2θ and has a relatively intense neutron beam, allowing the rapid collection of data. A neutron beam wavelength of 2.9592(2) Å was used, determined using the $La^{11}B_6$ NIST standard reference material 660b. The diffractograms were obtained with an exposure time of 5 min in the angular range 16.1–136.9° in 2θ during the charge–discharge cycling of the batteries. Sequential Rietveld refinements were carried out using the NPD data using Fullprof with visualization in WinplotR (Rodríguez-Carvajal, 1993; Roisnel and Rodriguez-Carvajal, 2000). The refinements were performed using data in the range 60–120° in 2θ.

III. RESULTS AND DISCUSSION

A. Crystallography and microstructure of the $Li_4Ti_5O_{12}$ anode

Using high-resolution NPD data, the crystallographic details of the anode was established. As reported by Pang *et al.* (2014a), the anode adopts $Fd\bar{3}m$ space-group symmetry, with a minor amount [1.9(3) wt%] of monoclinic Li_2TiO_3. The crystallographic details are summarized in Pang *et al.* (2014a). The as-prepared anode particles are cube-like with an average particle-size of ~200 nm.

B. *In situ* NPD

In situ NPD data of the battery are shown in Figure 3. In the absence of peak splitting in the NPD pattern for the cathode, we modeled the anode lattice evolution as single-phase $Li_{4+z}Ti_5O_{12}$ (solid-solution reaction) after Wagemaker *et al.* (2006), the details of which are presented in Pang *et al.* (2014a). The two-phase reaction between $LiFePO_4$ and $FePO_4$ in cathode is also observed in Figure 3.

To effectively refine the O positional parameter, it was necessary to fix the Li occupancy at 8*a* and 16*c* sites in the sequential Rietveld refinement, as per previous work (Pang *et al.*, 2014a, 2014b). Figure 4 summarizes the lattice and crystallographic changes occurring during battery cycling, including the variation of lattice parameter, O positional parameter, O–Ti–O bond angle (α), Ti–O bond length, and the estimated Ti oxidation state.

During charge, the anode lithiates and the lattice undergoes rapid expansion, followed by a gradual contraction. The non-linearity in the lattice response is attributed to the interplay of the amount and site of Li insertion (Sharma *et al.*, 2013; Pang *et al.*, 2014a), with the population of Li at the two crystallographic sites (i.e., 8*a* and 16*c*) having a different effect on the lattice. Interestingly, these lattice changes are not reflected in the trend of TiO_6 octahedral distortion, with no measureable distortion occurring during the initial lattice-expansion. We find that the gradual lattice-contraction, associated with population of Li at the 16*c* site in the anode (Pang *et al.*, 2014a), is strongly correlated to the trend of the TiO_6 distortion. The repositioning of the O atom in response to lithiation at the 16*c* site is important in maintaining the stability of the anode, and reflects the trend in the estimated oxidation-state of the Ti. As shown in Figure 4, during battery charge the O atom moves further away from the Ti atom, at (0.5, 0.5, 0.5), resulting in an increase in the length of the Ti–O bond that occurs alongside a decrease in the average Ti valence as estimated by the bond-valence summation (BVS) method (Brown and Altermatt, 1985). We note that the BVS method will yield an approximate Ti valence as the Ti shares the 16*d* site with Li. The ideal Ti^{4+}–O^{2-} bond-length of 1.815 Å and an empirical constant of 0.37 Å (Brown *et al.*, 1985) are used in this estimation. The bond angle or α also varies with the oxygen positional-parameter, characterizing the distortion of the TiO_6 octahedron (Figure 5). The TiO_6 octahedron deformation and distortion result in a stable structure during the lithiation and delithiation processes. Alongside the Li repositioning, it is the oxygen positional-parameter changes during battery charge and discharge that completes the picture of the $Li_4Ti_5O_{12}$ structural response and anode function.

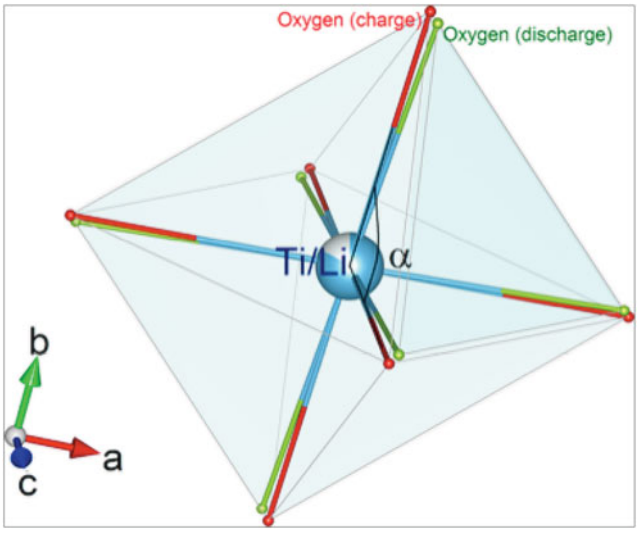

Figure 5. (Color online) Overlaid structures of the TiO_6 unit in the anode at the charged (O atom in red) and discharged (O atom in green) battery states showing that the O–Ti–O bond-angle (α) is larger at the charged state and smaller at the discharged state. All O atoms are crystallographically equivalent.

IV. CONCLUSION

We have successfully monitored the crystallographic change in the $Li_{4+z}Ti_5O_{12}$ anode within in a battery during charge and discharge. We report the details of the change to the TiO_6 structural unit occurring during Li diffusion that contributes to the structural stability of this "zero strain" anode. We find that while the initial expansion of the lattice upon lithiation is not reflected in the trend of TiO_6 octahedral distortion, the gradual lattice-contraction experienced during further lithiation is strongly correlated to the trend of the TiO_6 distortion, and associated with the repopulation of Li at the 16*c* site in the anode.

ACKNOWLEDGEMENTS

The authors acknowledge the travel support funded by National Synchrotron Radiation Research Center (2013-3-100-1). The research was supported by the Australian Nuclear Science and Technology Organization's (ANSTO) Energy Materials project. The authors are also grateful to Professor Lin, Jeng-Yu of Tatung University for providing $Li_4Ti_5O_{12}$

sample, Tatung Fine Chemicals Co., Taiwan for providing $LiFePO_4$ sample, and the staff members at the Bragg Institute, ANSTO for their operations support.

Brown, I. D. and Altermatt, D. (**1985**). "Bond-valence parameters obtained from a systematic analysis of the Inorganic Crystal Structure Database," Acta Crystallogr. B **41**, 244–247.

Cho, J., Kim, Y. J., Kim, T.-J., and Park, B. (**2001**). "Zero-strain intercalation cathode for rechargeable Li-ion cell," Angew. Chem. Int. Ed. **113**, 3471–3473.

Hunter, B. (**1998**) "Rietica - a visual Rietveld program". International Union of Crystallography Commission on Powder Diffraction Newsletter No. 20, (Summer) http://www.rietica.org

Liss, K.-D., Hunter, B., Hagen, M., Noakes, T., and Kennedy, S. (**2006**). "Echidna—the new high-resolution powder diffractometer being built at OPAL," Physica B 385–386, Part 2, 1010–1012.

Ohzuku, T., Ueda, A., and Yamamoto, N. (**1995**). "Zero-strain insertion material of $Li[Li_{1/3}Ti_{5/3}]O_4$ for rechargeable lithium cells," J. Electrochem. Soc. **142**, 1431–1435.

Pang, W. K., Peterson, V. K., Sharma, N., Shiu, J.-J., and Wu, S.-h. (**2014a**). "Lithium migration in $Li_4Ti_5O_{12}$ studied using *in situ* neutron powder diffraction," Chem. Mater. **26**, 2318–2326.

Pang, W. K., Sharma, N., Peterson, V. K., Shiu, J.-J., and Wu, S.-H. (**2014b**). "In-situ neutron diffraction study of the simultaneous structural evolution of a $LiNi_{0.5}Mn_{1.5}O_4$ cathode and a $Li_4Ti_5O_{12}$ anode in a $LiNi_{0.5}Mn_{1.5}O_4$‖$Li_4Ti_5O_{12}$ full cell," J. Power Sources **246**, 464–472.

Rodríguez-Carvajal, J. (**1993**). "Recent advances in magnetic structure determination by neutron powder diffraction," Physica B **192**, 55–69.

Ronci, F., Reale, P., Scrosati, B., Panero, S., Rossi Albertini, V., Perfetti, P., di Michiel, M., and Merino, J. M. (**2002**). "High-resolution in-situ structural measurements of the $Li_{4/3}Ti_{5/3}O_4$ "zero-strain" insertion material," J. Phys. Chem. B **106**, 3082–3086.

Sharma, N., Yu, D., Zhu, Y., Wu, Y., and Peterson, V. K. (**2013**). "Non-equilibrium structural evolution of the lithium-rich $Li_{1+y}Mn_2O_4$ cathode within a battery," Chem. Mater. **25**, 754–760.

Studer, A. J., Hagen, M. E., and Noakes, T. J. (**2006**). "Wombat: the high-intensity powder diffractometer at the OPAL reactor," Physica B **385–386**, Part 2, 1013–1015.

Roisnel, T. and Rodriguez-Carvajal, J. (**2000**). "WinPLOTR: a windows tool for powder diffraction patterns analysis," in Paper read at Materials Science Forum, Proc. of the Seventh European Powder Diffraction Conf. (EPDIC 7).

Tarascon, J. M. and Armand, M. (**2001**). "Issues and challenges facing rechargeable lithium batteries," Nature **414**, 359–367.

Wagemaker, M., Simon, D. R., Kelder, E. M., Schoonman, J., Ringpfeil, C., Haake, U., Lützenkirchen-Hecht, D., Frahm, R., and Mulder, F. M. (**2006**). "A kinetic two-phase and equilibrium solid solution in spinel $Li_{4+x}Ti_5O_{12}$," Adv. Mater. **18**, 3169–3173.